Magnetic Resonance in Medicine 45:521–524 (2001)

Efficient Off-Resonance Correction for Spiral Imaging

Krishna S. Nayak,* Chi-Ming Tsai, Craig H. Meyer, and Dwight G. Nishimura

A new spiral imaging technique incorporates the acquisition of a field map into imaging interleaves. Variable density spiral trajectories are designed to oversample the central region of *k*-space, and interleaves are acquired at two different echo times. A field map is extracted from this data and multifrequency reconstruction is used to form an off-resonance corrected image using the entire dataset. Simulation, phantom, and in vivo results indicate that this technique can be used to achieve higher image and/or field map spatial resolution compared to conventional techniques. Magn Reson Med 45: 521–524, 2001. © 2001 Wiley-Liss, Inc.

Key words: spiral MRI; off-resonance correction; *k*-space; reconstruction

Spiral imaging is used for a variety of applications due to its efficient *k*-space coverage (1) and excellent flow properties (2). In spiral imaging, however, off-resonance can result in image domain blurring (3). Conventional approaches to spiral off-resonance correction involve acquiring a field map using extra acquisitions. Typically, two low-resolution single-shot spiral images, taken at different echo times, are used to compute a field map. This map may then be used for linear field map correction or a frequency-sensitive reconstruction (4,5). Disadvantages of this approach are that separate field map acquisitions are required, magnitude information from the field map images are unused, and the field map resolution is not very flexible.

We present a new technique, termed ORC-VDS (off-resonance correction using variable density spirals) that combines the image and field map acquisitions using a variable density spiral (VDS) trajectory that oversamples the *k*-space origin. This technique has greater scan time efficiency relative to conventional techniques and enables the flexible tradeoff of field map resolution for image resolution.

A similar technique has been previously applied to projection reconstruction imaging (6) where the central *k*-space is inherently oversampled and off-resonance blurring occurs. In spiral imaging, oversampling the *k*-space origin requires trajectory modification, but the longer readouts make off-resonance blurring a more significant obstacle that requires accurate correction.

Department of Electrical Engineering, Stanford University, Stanford, California.

A preliminary account of this work was presented at the 8th Annual Scientific Meeting of the ISMRM, Denver, 2000 (abstract 116).

Grant sponsors: National Institutes of Health; GE Medical Systems.

*Correspondence to: Krishna S. Nayak, Packard 211, ISL, 350 Serra Mall, Stanford University, Stanford, CA 94305-9510.
E-mail: nayak@lad.stanford.edu

Received 16 May 2000; revised 31 August 2000; accepted 14 September 2000.

METHODS

In the proposed technique, variable density spiral (VDS) trajectories (see Fig. 1) are designed such that a small circular region around the *k*-space origin is oversampled by a factor of 2. Every alternate spiral acquisition is then delayed by a small amount labeled ΔTE. The 2× oversampled region is used to generate two lower-resolution images with different echo times—one from the early-TE interleaves and one from the late-TE interleaves. Notice that the low-resolution images have the same field of view (FOV) as an image from the full dataset.

A field map is then computed in the standard way, using the phase difference between the two low-resolution images. Since these field map estimates are only reliable in areas of sufficient signal, a smooth polynomial approximation (7) over the entire FOV can be computed for use during reconstruction.

A multifrequency image reconstruction is then used to simultaneously compensate for off-resonance and correct for the difference in echo times (4–6). In multifrequency reconstruction, a small finite set of frequency samples $\{\Delta f_n\}$ are selected such that they span the full range of off-resonant frequencies. For each Δf_n, an image is reconstructed based on that frequency of precession. This is done by modulating the raw data of each readout by $e^{+2\pi i \Delta f_n t}$ and phase-aligning the early and late echo data by multiplying the raw data from late-TE acquisitions by $e^{+2\pi i \Delta f_n \Delta \mathrm{TE}}$. An image is then generated via gridding reconstruction (8,9) with the modulated and aligned data from both early-TE and late-TE acquisitions. For the final image, each voxel is estimated by interpolating between the images based on the closest $\{\Delta f_n\}$ frequency samples to $\Delta f(x, y)$ (4) or by taking a linear combination of all the $\{\Delta f_n\}$ images (5).

Resulting images are formed without separate field map acquisitions and with only a moderate increase in reconstruction time. This combination of image and field map acquisitions provides for greater scan efficiency, while the ability to specify the oversampled region provides flexibility in trading off field map resolution for image resolution.

RESULTS

Performance comparisons and results are presented based on our scanner, a GE Signa 1.5T CV/i scanner (General Electric, Milwaukee, WI). This scanner is equipped with gradients capable of 40 mT/m magnitude and 150 T/m/sec slew rate and a receiver capable of 4 μsec sampling (±125 kHz). For phantom studies a head coil was used and for in vivo studies a body coil was used for RF transmission and 5-inch surface coil used for signal reception. Unless specified, all ORC-VDS images use a ΔTE of 1 msec.

Performance Evaluation

A first comparison of ORC-VDS against the conventional (separate field map) technique is illustrated in Fig. 2. Op-

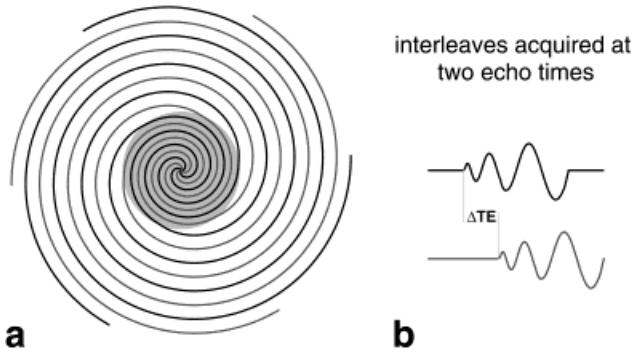

FIG. 1. ORC-VDS *k*-space trajectories: (**a**) VDS trajectories are designed to oversample a circular region around the *k*-space origin, (**b**) interleaves are acquired at two different echo times, and (**c**) two low-resolution images formed from the oversampled region are used to compute a field map. Note that the two low-resolution images have the same FOV as the full VDS dataset.

timal spiral and VDS trajectories (10–12) were designed based on 20 cm FOV, 16.384 msec readouts, and the full gradient and receiver capability of our scanner.

In Fig. 2a, ORC-VDS and the conventional technique are compared using six excitations. The bullet represents the field map resolution and image resolution achievable using four interleaves for the image and two field map acquisitions. The curved line represents the full range of field map and image resolutions that can be achieved with ORC-VDS simply by adjusting the size of the oversampled *k*-space region. Figure 2b contains identical comparisons for different numbers of excitations.

In all cases the ORC-VDS technique achieves higher image and field map resolution because all acquired data are used for both the image and the field map. In addition, the proposed technique enables greater flexibility in choosing field map resolution based on the expected off-resonance. For example, in the six-excitation case ORC-VDS can achieve either 10% higher image resolution with the same field map resolution or 20% higher field map resolution with the same image resolution; or, field map resolution can be traded off for up to a 40% increase in image resolution without additional scan time.

Experimental Results

To demonstrate this technique it was applied to the imaging of a resolution phantom with high-order off-resonance and to 2D coronary imaging with mostly linear off-resonance. Both experiments were conducted in a well-shimmed magnet with off-resonance within ± 35 Hz.

Figure 3 contains cropped images of a resolution phantom first scanned with conventional spirals (22 interleaves for the image and 2 excitations for the field map) and then ORC-VDS with the 24 interleaves designed to achieve higher field map resolution (with the same spatial resolution). All three images have 0.74-mm in-plane resolution over a 16-cm FOV. Both corrected images used multifrequency reconstruction using the field map; the conventional spiral image achieved 6.78-mm field map resolution, while the ORC-VDS image achieved 5.2-mm field map resolution with the same scan time. The ORC-VDS technique provided a 68% improvement in field map resolution (voxel area), which is apparent by the reduced blurring of the comb bristles even in this well-shimmed phantom.

Figure 4 contains 2D coronary images from ECG triggered breath-held studies on a normal volunteer. The vol-

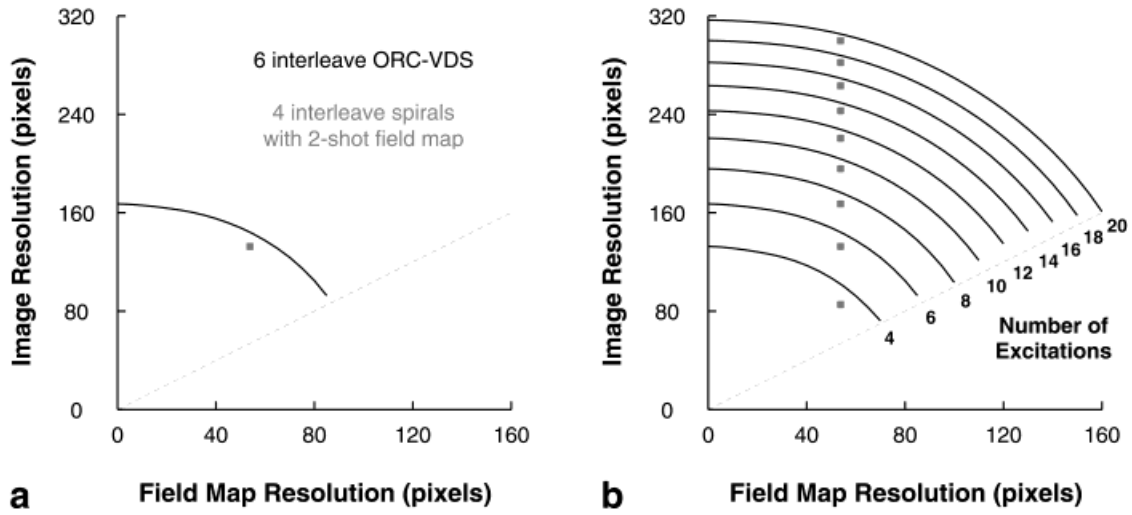

FIG. 2. Performance comparison of ORC-VDS and conventional techniques. **a:** Resolution comparison of six interleave ORC-VDS, and conventional four interleave spirals with a two-excitation field map. **b:** Similar comparisons for different numbers of excitations. Comparisons are based on a 20 cm FOV, 16.384 msec readouts, with 4 μsec sampling, and gradients supporting 40 mT/m magnitude and 150 T/m/sec slew rate.

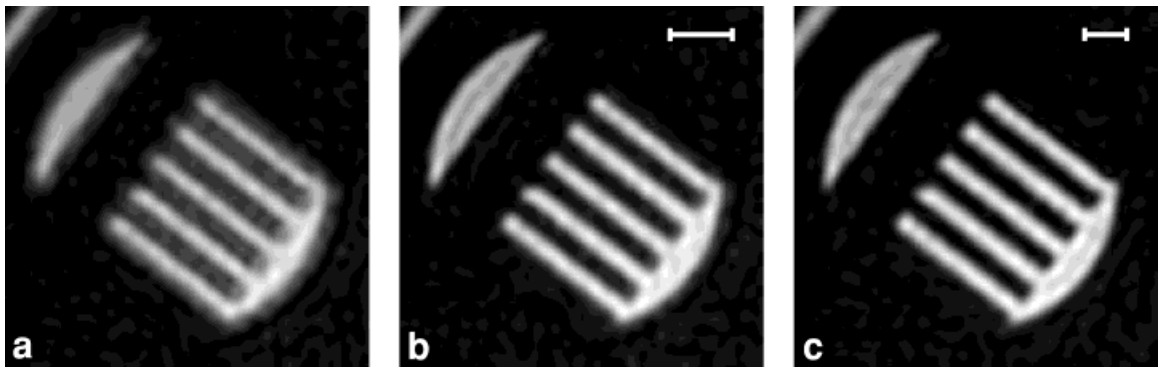

FIG. 3. Resolution phantom: Cropped images of a resolution phantom scanned with (**a**) 22 interleave spirals and no inhomogeneity correction, (**b**) 22 interleave spirals with a 2-excitation field map and multifrequency correction, achieving 6.78 mm field map resolution, and (**c**) 24 interleave ORC-VDS achieving 5.2 mm field map resolution. The ORC-VDS image is sharper than the conventional corrected spiral image acquired in the same scan time. White bars indicate field map spatial resolution in **b** and **c.**

unteer was first scanned with conventional spirals (12 interleaves for the image and two excitations for the field map) and then ORC-VDS with the 14 interleaves designed to achieve higher image resolution (sacrificing field map resolution). Over a 20-cm FOV, the conventional spiral image has 0.72-mm image resolution and 3.25-mm field map resolution, while the ORC-VDS image achieves 0.68-mm image resolution and 4-mm field map resolution. By permitting very low resolution field map correction, ORC-VDS enabled the same scan time to be used to achieve higher image resolution. Notice the improved vessel definition in Fig. 4b (shown by white arrows). In such cases higher image resolution may be more valuable than field map resolution.

DISCUSSION

In summary, VDS trajectories can be designed to oversample the *k*-space origin. Then by interleaving delayed and nondelayed acquisitions, a field map can be computed from the central portion of *k*-space. Finally, multifrequency reconstruction can be used to compensate for off-resonance artifacts. Simulations indicate that this technique achieves higher image and/or field map resolution compared to acquiring a field map in separate acquisitions. Phantom and in vivo studies demonstrate the inherent resolution gains and the benefits of freely trading off image and field map resolution. An additional benefit of this technique is the reduction of off-resonance artifacts in the field map, because the field map acquisition is spread out over all interleaves and is acquired over a smaller time window.

When imaging ultrashort T_2 species, mixed contrast is an issue. Images from the two echo times possess different contrast, which produce spiral-shaped aliasing artifacts when they are combined. In general, ORC-VDS is intended for areas where a small ΔTE does not significantly alter contrast.

This technique is best suited for applications that require short echo times, good flow and motion properties, and that suffer from off-resonance artifacts. While we present this technique within the context of 2D spiral imaging, simple implementations exist for many 3D trajectories such as 3DPR, 3D stacks of spirals, and 3D cones.

ACKNOWLEDGMENTS

K.S.N. gratefully acknowledges the support of a Fannie and John Hertz Foundation Graduate Fellowship.

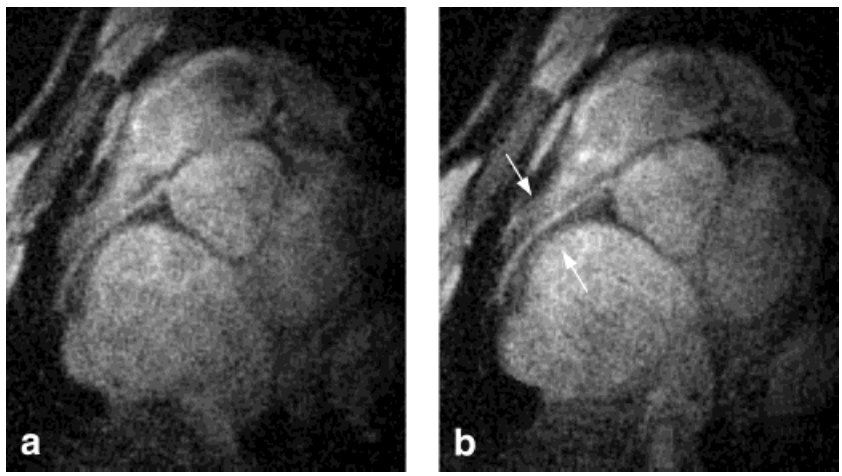

FIG. 4. Coronary images: Normal volunteer scanned with (**a**) conventional spirals with 12 image interleaves, two-excitation field map, and multifrequency correction, achieving 0.72 mm image resolution, and (**b**) ORC-VDS with 14 interleaves trading off field map resolution for 0.68 mm image resolution. The higher-resolution ORC-VDS image shows improved vessel definition (indicated by white arrows).

REFERENCES

1. Meyer CH, Hu BS, Nishimura DG, Macovski A. Fast spiral coronary artery imaging. Magn Reson Med 1992;28:202–213.
2. Nishimura DG, Irarrazabal P, Meyer CH. A velocity *k*-space analysis of flow effects in echo-planar and spiral imaging. Magn Reson Med 1995; 33:549–556.
3. Yudilevich E, Stark H. Spiral sampling in magnetic resonance imaging—the effect of inhomogeneities. IEEE Trans Med Imaging 1987;6: 337–345.
4. Noll DC, Meyer CH, Pauly JM, Nishimura DG, Macovski A. A homogeneity correction method for magnetic resonance imaging with time-varying gradients. IEEE Trans Med Imag 1991;10:629–637.
5. Man L-C, Pauly JM, Macovski A. Multifrequency interpolation for fast off-resonance correction. Magn Reson Med 1997;37:785–792.
6. Nayak KS, Nishimura DG. Automatic field map generation and off-resonance correction for PR imaging. Magn Reson Med 2000;43:151–154.
7. Luk Pat GT, Kerr AB, Nishimura DG. Inhomogeneity correction for echo-planar imaging with a polynomial estimate of the field map. In: Proc SMR, 3rd Annual Meeting, Nice, August, 1995. p 617.
8. O'Sullivan JD. A fast sinc function gridding algorithm for Fourier inversion in computer tomography. IEEE Trans Med Imaging 1985;4: 200–207.
9. Jackson JI, Meyer CH, Dwight AM, Nishimura G. Selection of a convolution function for Fourier inversion using gridding. IEEE Trans Med Imaging 1991;10:473–478.
10. Tsai C-M, Nishimura DG. Reduced aliasing artifacts using variable-density *k*-space sampling trajectories. Magn Reson Med 2000;43:452–458.
11. King KF, Foo TKF, Crawford CR. Optimized gradient waveforms for spiral scanning. Magn Reson Med 2000;34:156–160.
12. Meyer CH, Pauly JM. A rapid method of optimal gradient waveform design for *k*-space scanning in MRI. U.S. Patent Number 6,020,739; 2000.